



Photodegradation for Mordant Orange 37 and Direct Green B from Water using Nanokaolin

Sabah S. Ibrahim and Belal N.A. Mahran

Chemistry Department, Central Lab for Environmental Quality Monitoring, National Water Research Center, Delta Barrages, Egypt

Abstract

Increasing concentrations of dyes including mordant orange37 and direct green B in surface and groundwater are a major environmental concern in recent years. In this research, the potential of nanokaolin for efficient removal of MO37 and DGB residue from aqueous solutions was investigated. For this purpose, nanoKaolin was characterized by XRD, surface area and TEM techniques. Effect of various parameters such as contact time, adsorbent dosage, initial concentration of MO37 and DGB and temperature on adsorption of MO37 and DGB on nanokaolin was investigated. The results showed that the best condition for removal of MO37 and DGB was exhibited at contact time 90 min and adsorbent dosage 1g/L. The removal of MO37 and DGB decreased with the increase of initial concentration. Langmuir and Freundlich isotherm models were applied to the equilibrium data. Results indicate the potential of nano kaolin for removal of MO37 and DGB from aqueous solutions.

Received; 20 April, 2017, Revised form; 27 Jun. 2017, Accepted; 4 July. 2017, Available online 4 July, 2017

1. Introduction

Studies were undertaken for the removal of colour from different types of synthetic dye solutions by using powdered activated carbon (PAC) and bentonite clay (BC) as adsorbents [1].

The availability of safe and clean drinking water is decreasing day by day. To overcome this difficulty, Nanotechnology has been undertaken to explore various efficient ways for treatment of waste water in a more precise and accurate way with the support of various nanomaterials. Nanoparticles (NPs) have huge potential that enables them to participate in waste water treatment and/or water purification technologies. Their exclusive features such as high surface area, high mechanical properties, greater chemical reactivity, lower cost and energy, allow them to eliminate precisely toxic metal ions, viruses, bacteria, organic and inorganic solutes from the waste water. Different types of nanomaterials such as metal nanoparticles, nanosorbents, bioactive nanoparticles, nanofiltration (NF) membranes; carbon nano tubes (CNTs), zeolites and clay are proved to be efficient materials for waste water treatment [2].

Conventional adsorption systems generally use activated carbon [3, 4], which is expensive and necessitates regeneration. Because activated carbon [5] has a strong affinity for binding organic substances, even at low concentrations, it is very effective in treating organic-laden wastewaters.

Experimental investigations were carried out using commercially available kaolin to adsorb two different toxic cationic dyes namely crystal violet and brilliant green from aqueous medium. Kaolin was characterized by performing particle size distribution, BET surface area measurement and XRD analysis. The effects of initial dye concentration, contact time, adsorbent dose, stirring speed, pH, salt concentration and temperature were studied in batch mode. The extent of adsorption was strongly dependent on pH of solution. Free energy of adsorption (ΔG_0), enthalpy (ΔH_0) and entropy (ΔS_0) changes were calculated. Adsorption kinetic was verified by pseudo-first-order, pseudo-second-order and intra-particle-diffusion models [6]. The difficulty in the reuse or disposal of PAC is that being a very fine powder, it remains suspended for a long time in the treated water. The proper disposal, regeneration or reuse [7] of waste sludge has become a significant environmental issue.

Dyes represent one of the problematic groups. Currently, a combination of biological treatment and adsorption on activated carbon is becoming more common for removal of dyes from wastewater. Although commercial activated carbon is a preferred sorbent for color removal, its widespread use is restricted due to high cost. As such, alternative non-conventional sorbents have been investigated. It is well-known that natural materials, waste materials from industry and agriculture and biosorbents can be obtained and employed as inexpensive sorbents [8]. Reactive azo dyes are becoming more

popular in the textile industry; they are mainly used for cotton dyeing. However, reactive dyes hydrolyze easily, resulting in a high portion of unfixed (or hydrolyzed) reactive dyes, which have to be washed off during the dyeing process. As much as 50% of the initial dye load is present in the dye bath effluent [9]. Physico-chemical methods are applied for the treatment of these kinds of wastewaters, achieving high dye removal efficiencies [10].

Dye discharge from textile industries causes a serious threat to the water resources. Many different and complicated molecular structures of dyes make dye wastewater difficult to be treated by conventional methods [11].

Azo dyes, containing one or more azo bond (-N=N-), account for 60-70% of all textile dyestuffs used [12]. It is estimated that about 10- 15% of the total production of colorants is lost during their synthesis and dyeing Processes [13, 14]. Colored industrial effluent is the most obvious indicator of water pollution and the discharge of highly colored synthetic dye effluents is aesthetically displeasing and cause considerable damage to the aquatic life [15].

Textile industry has been considered for years to be one of the major sources of worldwide pollution problems. Huge amount of wastewater is generated at different stages of textile manufacturing. These waste products are mostly released in the environment without prior consideration. In Fact, they are highly contaminated with lot of chemicals including dyes [16].

Extensive literature information about dyes, its classification and toxicity, various treatment methods, and dye adsorption characteristics by various adsorbents have been studied. One of the objectives of the studies is to organise the scattered available information on various aspects on a wide range of potentially effective adsorbents in the removal of dyes. Therefore, an extensive list of various adsorbents such as natural materials, waste materials from industry, agricultural by-products, and biomass based activated carbon in the removal of various dyes has been shown [17]. Textile dyes extensively used in several manufacturing process have been proved to be harmful to the human health as well as to the environment. Moreover, these chemicals, especially the azo dyes, could raise potential environmental concerns considering their toxic, mutagenic and carcinogenic effects [18-20]. the availability of safe and clean drinking water is decreasing day by day. To overcome this difficulty, Nanotechnology

has been undertaken to explore various efficient ways for treatment of waste water in a more precise and accurate way with the support of various nanomaterials. Nanoparticles (NPs) have huge potential that enables them to participate in waste water treatment and/or water purification technologies. Their exclusive features such as high surface area, high mechanical properties, greater chemical reactivity, lower cost and energy, allow them to eliminate precisely toxic metal ions, viruses, bacteria, organic and inorganic solutes from the waste water [21].

The main objective of the work is to remove different concentrations of azo-dyes from industrial waste water using photodegradation.

2. Experimental Setup

2.1. Chemical and Reagents

All chemicals used in experiment were of analytical grade. preparation mordant orange37 and direct green B are 0.5×10^{-3} g/L. kaolin is using 0.1g/100ml .

Apparatus

TEM spectra were recorded by JSM-6380LA scanning electron

X-ray diffraction spectra were recorded by microscope (Jeol) Altima 4 X-Ray diffraction (Rigaco).

The characterization of kaolin - TEM (30-60 nm). Fig (1).

The characterization of the assessed azo-dyes. Table 1

2.2. Kaolin Nanoparticles

2.2.1. Preparation of Kaolin Nanoparticles

Nanokaolin is a product of kaolin, also known as white clay. Kaolin was established as supplementary cementitious material in concrete. The inclusion of kaolin in concrete enhances strength and durability and prolongs concrete life span. Nanokaolin can be developed by using sol gel technique which involves high energy milling [650-750 °C]. The process of milling been influenced by time of milling, ball and jar type. Ceramic type Zirconia has been used as jar and ball type in this process. Time of milling was set from four hours to one day. Sample was analyzed by using particle size analyzer to determine the particle size and surface area of kaolin. From the results it has been shown that the optimum milling period for nanoKaolin is one day base on particle size compared to 4 hours. Furthermore, one day milling produces a massive increment of surface area compare to others. In conclusion, one day can be considered as the optimum cycle time in the production of nanokaolin [22].

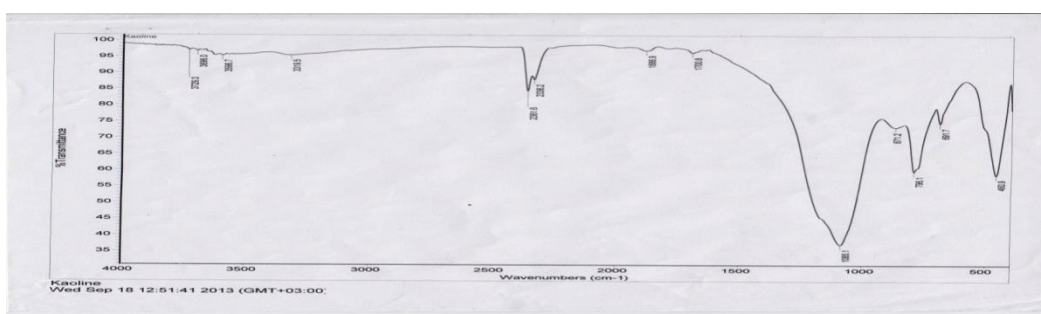


Fig (1): FTIR for Kaolin nanoparticles



Fig (2): XRD for Kaolin nanoparticles

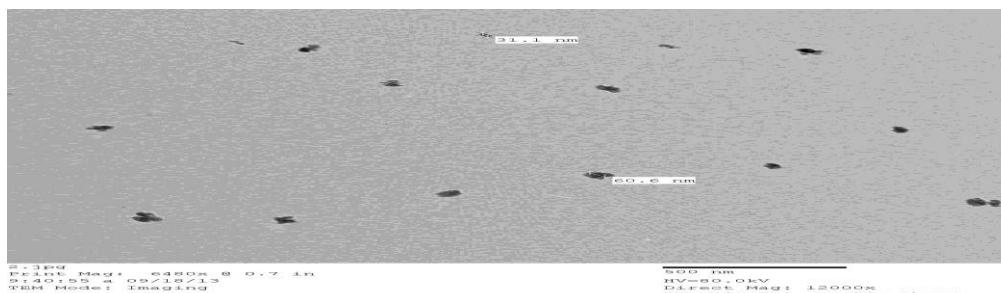


Fig (3): TEM for Kaolin nanoparticles

Table 1: Assessed Dyes

No.	Name	Molecular Formula	Mol. Weight	Molecular Structure
1	Mordant Orange 37	C ₁₆ H ₁₃ N ₄ NaO ₅ S	396.35	
2	DIAMINE GREEN B “Direct Green B”	C ₃₄ H ₂₂ N ₈ Na ₂ O ₁₀ S ₂	812.7	

2.2.2. Batch experiments

The batch experiments were carried out in 250 ml Erlenmeyer containing 100 ml of aqueous solution. The suspension was shaken in temperature controlled shaker at 200 rpm. The residual concentration of Mordant Orange37 and Direct Green B in supernatant was analysed by HACH UV-spectrophotometer. Effects of adsorbent dosage (0.1-0.4 g/L), contact time (10-60 min), initial MO37 and DGB concentration (0.031–1*10⁻³ g/L) and temperature (30 C⁰-70 C⁰) on photo degradation of MO37 and DGB by nanokaolin were investigated. The adsorption capacity q_e (mg/g) of the adsorbent was calculated from the following equations:

$$q_e = (C_i - C_e)V / W \quad (1)$$

$$R\% = (C_i - C_e) 100 / C_i \quad (2)$$

Where C_e is the residual concentration reached at equilibrium state, C_i is initial mordant orange37 and direct green B concentration, V is the volume of solution (L), W is the weight of adsorbent (g) and R% is the removal percentage.

3. Results and Discussion

3.1. Charaterization of Kaolin Nanoparticles

A systematic characterization on kaolin has been performed by FT-IR, XRD and TEM. The FT-IR spectrum of nanokaolin is shown in Fig (1).The two absorption peaks at wavelength of 1085 cm⁻¹ and 460cm⁻¹ indicate the formation of nanoparticles. Fig (2) shows the powder

XRD pattern of nanokaolin samples under ambient condition. The broad peak reveals the existence of an amorphous phase Kaolin. The characteristic broad peak at 12 θ to 68 θ indicates that nanoKaolin is predominately present in the sample. Fig (3) shows the TEM image of freshly synthesized Kaolin nanoparticles. It could be observed that the kaolin is in the form nanospheres, which exists in a diameter of 31- 60 nm.

3.2. Effect of contact time in presence of UV only

During direct photolysis, photon absorption gives rise to compounds in excited electronic states that are susceptible to chemical transformation. In UV direct photolysis, the contaminant to be destroyed absorbs the incident radiation and undergoes degradation starting from its excited state [23]. UV irradiation would attack and decompose some organic molecules by bond cleavage and free radical generation, but usually at very slow rates [24].

In the presence of UV radiation, the rate of dye removal is high for dye in the beginning. The removal reached its

maximum value at about 60 min for DGB (97%). The percent of removal is high for MO37 (99%). DGB in the beginning due to a larger surface area of the adsorbent being available for the adsorption of the dye. The equilibrium time for this dye was about 60 min. The removal percent at equilibrium was 97% for DGB and MO is 100%. The two stages sorption mechanism with the first rapid and quantitatively predominant and the second slower and quantitatively insignificant, has been extensively reported in literature [25]. A photochemical reaction is characterized by an activation related to the absorption of at least one photon by a molecule. The range of wavelengths generally used in photochemistry is in the UV/visible region (wavelength 200 to 700 nm). However, this is not always sufficient for suitable pollutant remediation. Thus, oxidants such as O₃, H₂O₂ and/or a catalyst are often used.

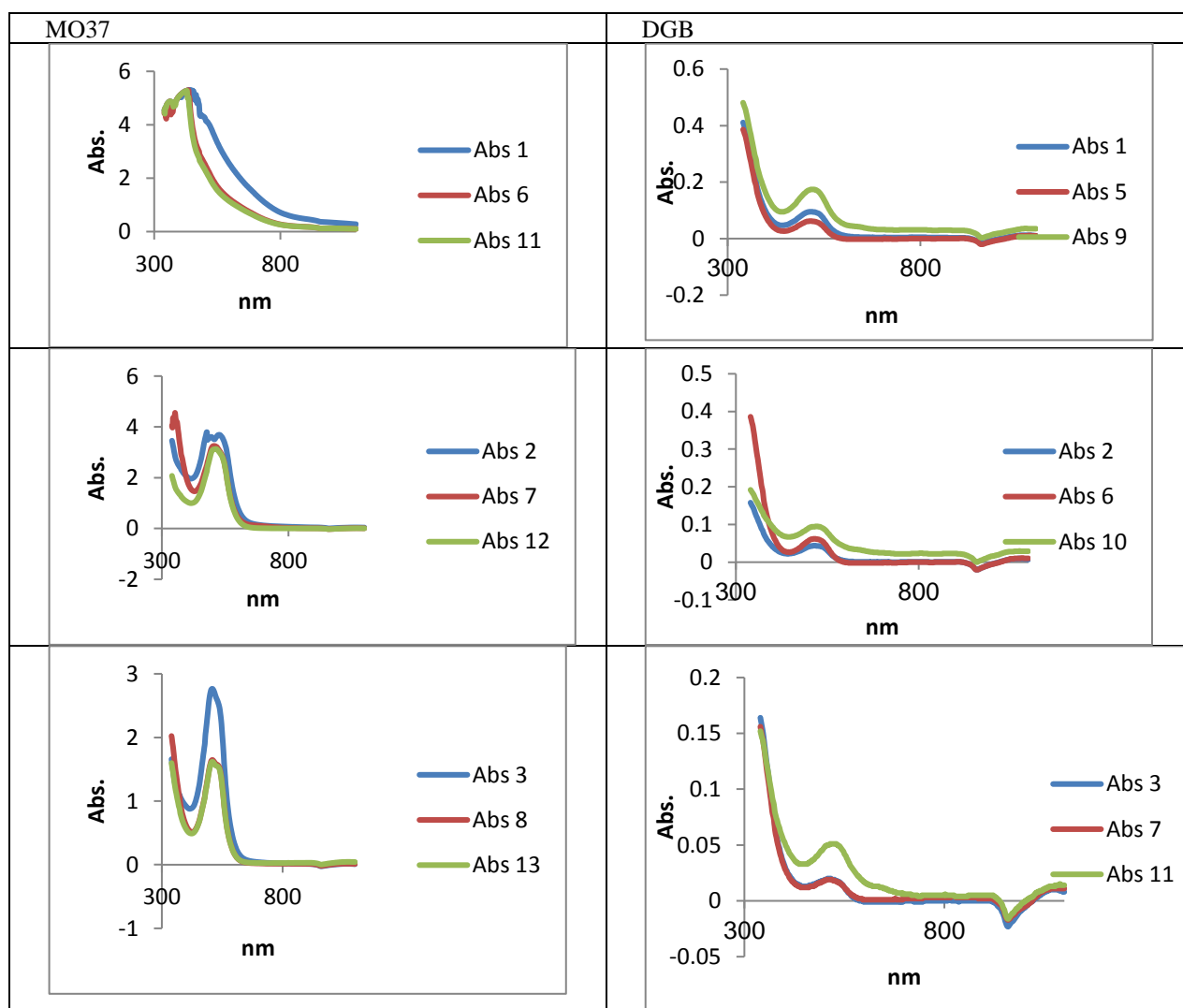
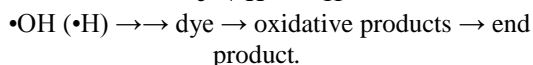
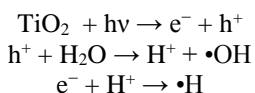


Fig (4): Effect of contact time in present of UV only

The mechanism of nanoTiO₂ photo catalysis is concluded as follows: TiO₂ absorbs UV light to generate electron (e⁻) and hole (h⁺). The holes combine with H₂O

on the surface of TiO₂ to form H⁺ and ·OH free radicals. H⁺ and electron react to yield ·H. The ·H and ·OH free radicals attack the organic molecule, and then produce

some intermediate products. The mechanism of photocatalytic degradation under UV light irradiation is described by [26]:



When the dye solutions exposed to the UV radiation in the presence of different nano particles under investigation, We take different concentration of MO37 and DGB Abs (1,2,3) represent concentration ($1 \cdot 10^{-3}$, $0.5 \cdot 10^{-3}$, $0.25 \cdot 10^{-3}$) concentration Abs1 before, Abs6 concentration after added kaolin ,Abs11 in present kaolin

and UV. We observed that the third case photo degradation is faster than the two other cases as shown in Fig (4).

3.3. Effect of contact time in present kaolin and UV lamp

When kaolin nanoparticles were used as photocatalyst in present UV lamp, the percent of MO37 removal was high to (99%) and DGB (97%). The experiments were performed until 60 min for all nanokaolin. The rate of removal is increase in the beginning due to a larger surface area of the adsorbent being available. The relation between removal percent for two dyes under consideration and contact time is shown in Fig (5).

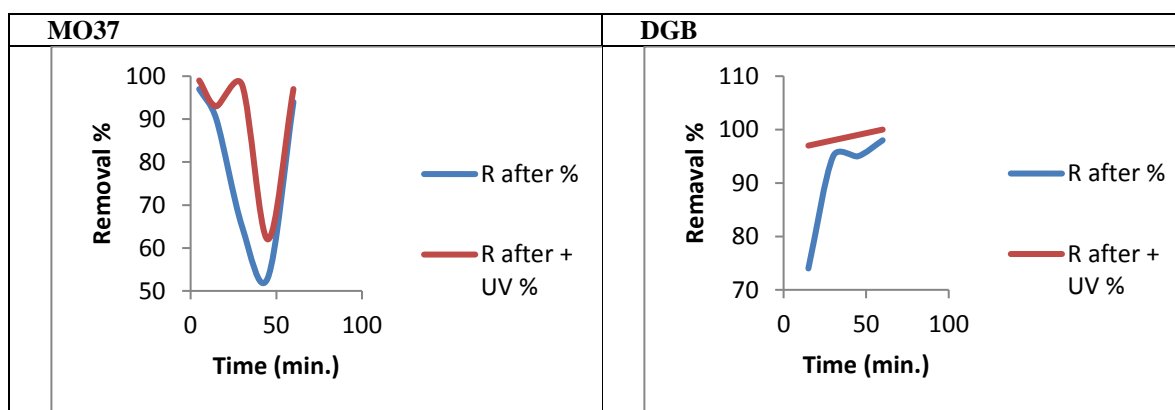


Fig (5): Effect of contact time in present kaolin and UV lamp

3.4. Effect of different dose from nanokaolin

Fig (6) illustrates the effect of different amounts of nano kaolin (0. 2 to 0.4 g for 100 ml) on the removal of MO37 and DGB It is observed that the efficiency of removal increased from 81% at 10 min but reach removal% to 95% at 90 min for MO37 while DGB efficiency of removal increase from 87% at 10 min. However, reach removal% to 97% at 90 min. however when using UV lamp increase photo degradation to reach removal% for MO37 to 99% at 30 min and reach to equilibrium state the removal% to 94% at use 0.2g of nanokaolin. Another state when using 0.3 g of nano kaolin the removal% of MO37 reach to 30% at 10 min but when using UV lamp increase photo

degradation and reach removal % for MO37 to 65% at 60 min. Another case when using 0.4 g of nanokaolin removal% reach to 25% at 30 min and reach to equilibrium state the removal% to 60% for MO37 but DGB removal% reach to 87% at 10 min and reach to equilibrium state the removal% to 97% at use 0.2g of nanokaolin. another state when using 0.3 g of nanokaolin the removal% of DGB reach to 93% at 10 min but when using UV lamp increase photo degradation and reach removal % for DGB to 98% at 60 min. Another case when using 0.4 g of nanokaolin removal% reaches to 94% at 10 min and reach to equilibrium state the removal% to 99 % at 60 min.

Table 2: Effect of different dose

Azo-Dye	Time (min.)	Conc. (gm)		
		0.2	0.3	0.4
MO37	30	99	65	25
	60	---	75	60
	90	94	---	---
DGB	10	87	93	94
	60	97	98	99

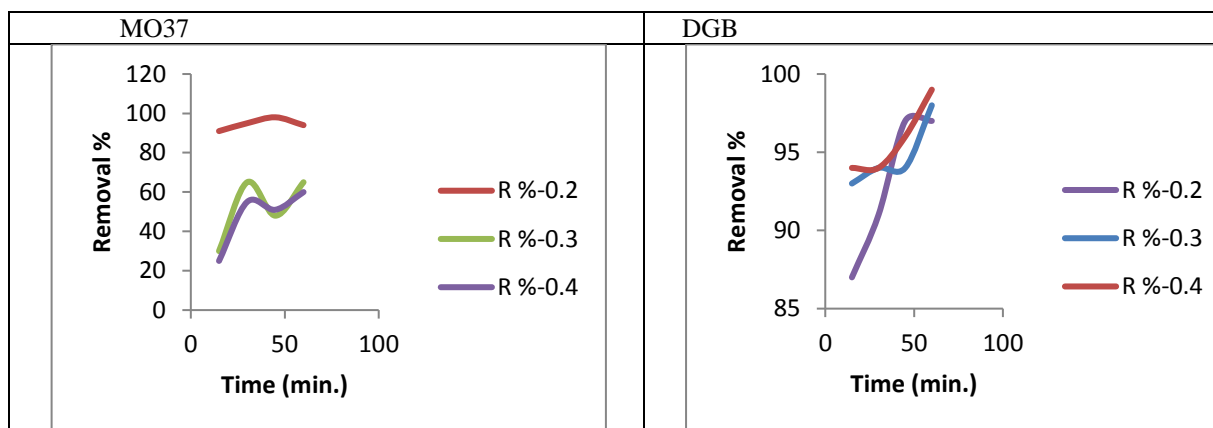


Fig (6): Effect of different dose from nanokaolin

3.5. Effect of Initial Dye Concentration on Dye Uptake

The dye uptake mechanism is particularly dependent on the initial dye concentration: at low concentrations, dyes are adsorbed by specific sites, while with increasing dyes concentrations the specific sites are saturated and the exchange sites are filled. It is observed that with increasing initial concentrations, the adsorption capacity increases while the percent dyes removal decreases. Though an increase in dye uptake was observed, the decrease in percentage adsorption may be attributed to lack of sufficient surface area to accommodate much more dyes available in the solution. At lower concentrations, the dye present in solution could interact with the binding sites and thus the percentage adsorption was higher [27]. The general shapes of the isotherms are similar for different biomasses. However, the adsorption capacities and affinities are significantly different.

In the same time, literature showed that adsorption is independent of the contaminant concentration, and in some cases, the rate is lowered with increased initial concentration [28]. Different explanations were proposed,

all of which rely on the adsorption of contaminant molecules on the solid surface. One explanation assumed that at higher contaminant concentration, the contaminant molecules may compete with the adsorbed intermediates and inhibit degradation [29].

3.6. Effect of dyes concentration removal by nanokaolin in present UV lamp

The effect of initial dyes concentration on the rate of dyes uptake onto nanokaolin was studied using batch agitation in 250 ml beakers containing dye solutions of initial concentrations ranging from 1×10^{-3} to 0.031 mg L^{-1} , agitated at 250 rpm and at room temperature ($25 \pm 1^\circ\text{C}$) without any change in the initial pH of the test solution. The equilibrium concentration was evaluated after 90 min of contact time. The photo degradation for dye data presented in Fig (7) indicate that the percentage removal of MO37 and DGB decreases with increase in initial MO37 and DGB concentration, thus explaining the effect of UV lamp making photo degradation for MO37 and DGB to reach maximum removal% reach up to 98% and 66% at equilibrium for DGB and MO37 respectively.

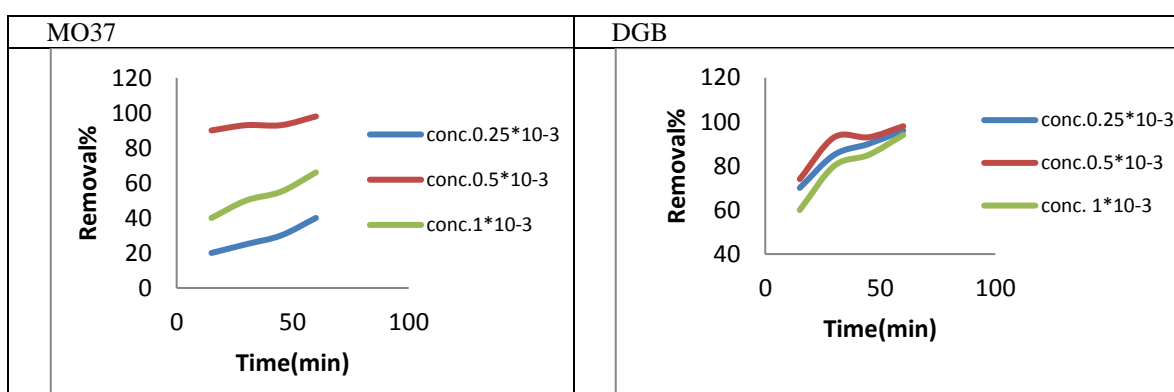


Fig. (7): Effect of dyes concentration removal by nanokaolin in present UV lamp

3.7. Effect of PH in photo degradation of MO37 and DGB in present UV lamp

Effect of PH on photo degradation of MO37 and DGB on surface of nanokaolin are variable ,but give maximum

degradation at natural PH =1 for DGB reach removal % to 96% and MO37 reach removal % to 93% at PH =2 in Fig (8).

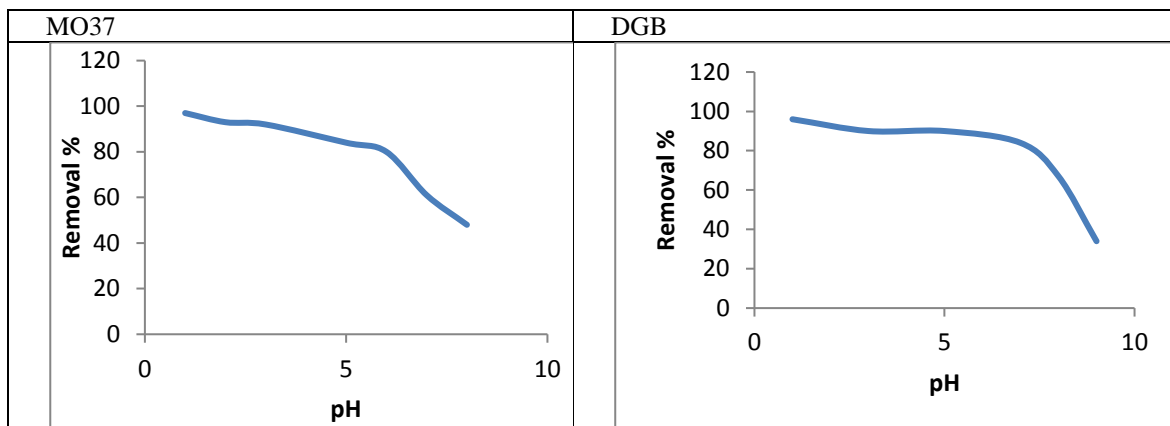


Fig (8): Effect of PH in photo degradation of MO37 and DGB in present UV lamp

3.8. Effect of temperature for removal DGB and MO37 in present UV lamp

The temperature of the medium could be important for energy-dependent mechanisms in the removal efficiency by different materials. The reason of this effect is thought to be the fact that temperature is an important factor affecting the adsorption and photo catalysis. In the case of photo catalytic process, the photo catalytic degradation rate increases with increasing temperature. In other words, higher temperature provides higher electron transfers in valance bond to higher energy levels and hence facilitating the electron-hole production that could be utilized in

initiating oxidation and reduction reactions [30]. The species photon-generated holes, and electrons, and hydroxyl radicals ($\bullet\text{OH}$) can thus degrade organic pollutant to intermediates, and then the intermediates are further degraded to CO_2 and H_2O .

In general, the activated energy of photo catalytic reaction is slightly affected by the temperature, but consecutive redox reaction may be largely influenced by temperature which affects both collision frequency of molecules and adsorption equilibrium [31]. So the overall effect on the photo catalytic performance will depend on the relative importance of these phenomena.

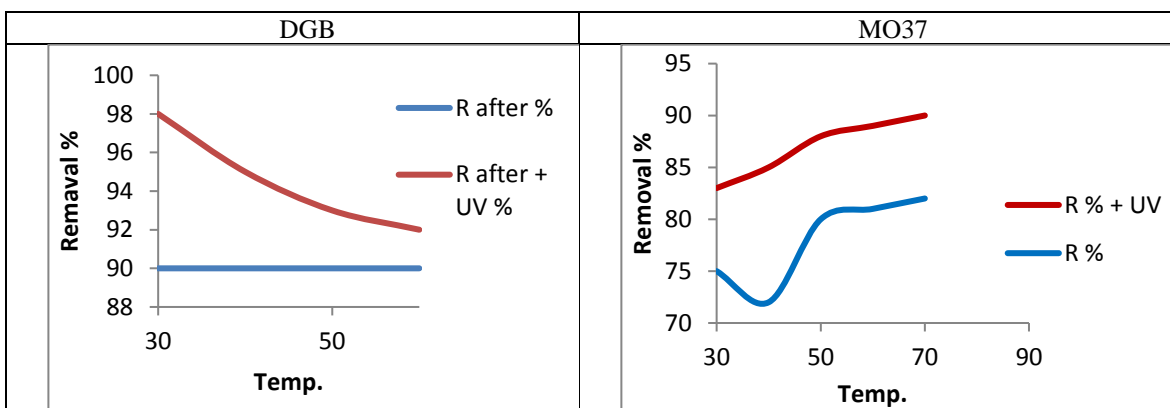


Fig (9): Effect of temperature (C°) for removal MO37 and DGB in present UV lamp

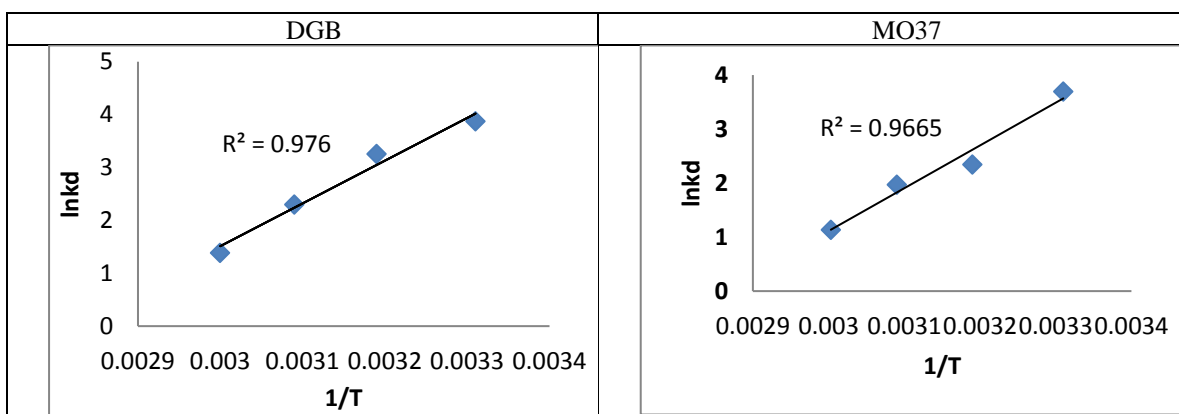


Fig (10): Effect of temperature on removal MO37 and DGB using nanokaolin

Table 3: Effect of temperature on removal for DGB

T	1/T	Removal%	K _D	ln K _D	R ²
303	3.30x10 ⁻³	97.70	48	3.87	0.976
313	3.195x10 ⁻³	95	26	3.258	intercept = -22.6479 slope = 7920.2
323	3.096x10 ⁻³	93	10	2.30	
333	3.003x10 ⁻³	92	4	1.38	

Table 4: Thermodynamic parameters for DGB

ΔH kJ/mol	ΔS J/mol	ΔG kJ/mol			
		303 k	313 k	323 k	333 k
-67208.4	-189.053	-9.749	-8.457	-6.17	-3.820

Table 5: Effect of temperature on removal for MO37

T	1/T	Removal%	K _D	ln K _D	R ²
303	3.30x10 ⁻³	83	40.2	3.69	0.9672
313	3.195x10 ⁻³	85	10.4	2.34	Intercept= -22.7391 Slope = 8083.758
323	3.096x10 ⁻³	88	7.2	1.97	
333	3.003x10 ⁻³	92	3.12	1.13	

Table 6: Thermodynamic parameters for MO37 .

ΔH kJ/mol	ΔS J/mol	ΔG kJ/mol			
		303 k	313 k	323 k	333 k
-65848.6	-188.295	-9.303	-6.89	-5.353	-3.165

In order to evaluate the thermodynamic feasibility of the removal process and to confirm the nature of the adsorption process, thermodynamic parameters (ΔG°, ΔH° and ΔS°) were calculated from the following equations [5,6]:

$$K_D = \frac{C_{Ad}}{C_e} \quad (4)$$

$$\Delta G = -RT \ln K_D \quad (5)$$

$$\ln K_D = -\left(\frac{\Delta H}{RT}\right) + \frac{\Delta S}{R} \quad (6)$$

where K_D is the equilibrium constant, C_{Ad} (mg/L) is the concentration of the dye adsorbed on solid at equilibrium, C_e (mg/L) is the equilibrium concentration of dye in the solution, R is the universal gas constant, 8.314 J/mol⁻¹/K, T is the absolute temperature in K, and the value of K_D in can be obtained from the adsorption percent at equilibrium. The values of ΔH and ΔS can be obtained from the slope and intercept of a van't Hoff plot of ln K_D versus 1/T as seen in Fig. and the thermodynamic parameters for adsorption of DGB and MO37 on kaolin are listed in Tables 4-6.

4. Adsorption Isotherms

The adsorption isotherm indicates how the adsorption molecules distribute between the liquid phase and the solid phase when the adsorption process reaches an equilibrium state. The analysis of the isotherm data by fitting them to different isotherm models is an important step to find the suitable model that can be used for design purpose. The isotherm data were fitted to the Langmuir and Freundlich isotherms.

4.1. The Langmuir Model

The Langmuir adsorption isotherm has been successfully applied to many pollutants adsorption processes and has been the most widely used sorption isotherm for the sorption of a solute from a liquid solution [32]. The saturated monolayer isotherm can be represented as:

$$q_e = \frac{Q_0 b C_e}{1 + b C_e}$$

The above equation can be rearranged to the common linear form:

$$\frac{C_e}{q_e} = \frac{1}{Q_0 b} + \frac{C_e}{Q_0}$$

where C_e is the equilibrium concentration(mg/L); q_e is the amount of dye adsorbed per unit mass of adsorbent (mg/g); Q₀ is q_e for a complete monolayer (mg/g), a constant related to sorption capacity; and b is a constant

related to the affinity of the binding sites and energy of adsorption (L/mg). A high *b* value indicates a high affinity. The values of *Q*₀ and *b* were for all adsorbents determined respectively from intercept and slopes of the linear plots of *C*_e/*q*_e vs. *C*_e.

The essential characteristics of Langmuir isotherm can be expressed by a dimensionless constant called equilibrium parameter *R*_L, defined by [33]:

$$R_L = \ln K_F + \frac{1}{n} \ln C_e$$

The value of *R*_L indicates the type of the isotherm to be either unfavorable (*R*_L > 1), linear (*R*_L = 1), favorable (0 < *R*_L < 1) or irreversible (*R*_L = 0).

4.2. Langmuir Adsorption Isotherm for nanokaolin

The different adsorption parameters for adsorption of MO37 and DGB are collected in Table 7. These parameters are *C*₀, *C*_e, ln *C*_e, *q*_e, ln *q*_e and *C*_e/*q*_e. The plot of *C*_e vs. *C*_e/*q*_e gave straight lines for all dyes Fig (11), from their slopes and intercepts, the values of *Q*₀ and *b* could be evaluated, respectively.

Table 7: Adsorption parameters for MO37 on nanokaolin

Azo-Dye	<i>C</i> ₀	<i>C</i> _e	ln <i>C</i> _e	<i>q</i> _e	ln <i>q</i> _e	<i>C</i> _e / <i>q</i> _e
MO37	0.001	0.00042		0.00022		
		8		9		
		0.00308	-7.756	0.00076	-8.382	1.868
		4	-5.781	6	-7.173	4.024
		5.14E-05	-9.876	1.95E-05	-10.847	2.638
		0.0001		05		
0.00006	2.73E-05	-10.509	1.31E-05	-11.243	2.083	
0.00003	05	-10.488	05	-12.235	5.735	
		2.79E-05		4.86E-06		

Table 8: Adsorption parameters for DGB on nanokaolin

Azo-Dye	<i>C</i> ₀	<i>C</i> _e	ln <i>C</i> _e	<i>q</i> _e	ln <i>q</i> _e	<i>C</i> _e / <i>q</i> _e
DGB	0.001	8.583E-06		0.00039		
		7		7		
		0.00199	-11.665	0.00199	-7.832	0.0216
		9	-13.434	9	-6.214	0.0007
		2.91E-05	-10.509	2.91E-05	-10.445	0.937
		0.0001		05		
0.00006	0.0000487	-9.9288	4.5E-06	-12.311	10.833	
0.00003	0.000052	-9.8642	-8.8E-06	----	-5.909	

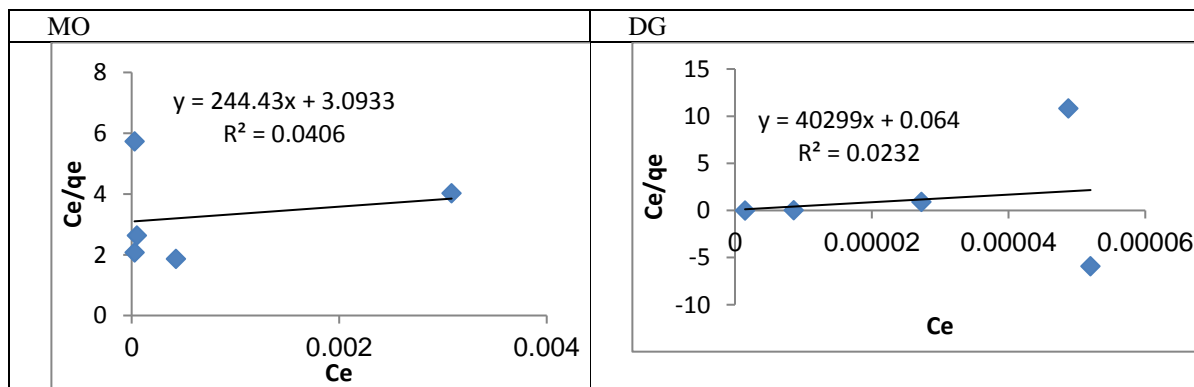


Fig (11): Langmuir isotherm for MO37 and DGB with nanokaolin

The data obtained for slope, intercept, *Q*₀ and *b* are shown in Table 9. The applicability of the model was examined by evaluating the correlation coefficient (*R*).

The higher the values of *R*, the more applicable the model for the dye examined.

Table 9: Langmuir equation parameters for nanokaolin

Azo-Dye	Slope	Intercept	Q_0	b	R^2
MO	244.4	3.093	0.00409	79.017	0.040
DG	40.29	0.064	0.02482	629.53	0.023

4.3. The Freundlich Model

On the other hand, the Freundlich isotherm assumes that the adsorption occurs on heterogeneous surface at sites with different energy of adsorption and with non-identical adsorption sites that are not always available. Mathematically it is characterized by the heterogeneity factor ‘1/n’[34]. Freundlich model can be represented by the linear form as follows:

$$\ln q_e = \ln K_F + \frac{1}{n} \ln C_e$$

where K_F is the Freundlich constant (mg/g)/(L/mg)ⁿ and n is the heterogeneity factor. The K_F value is related to the adsorption capacity; while $1/n$ value is related to the adsorption intensity. A plot of $\ln q_e$ versus $\ln C_e$, gives a straight line with K_F and $1/n$ determined from the intercept and the slope, respectively.

4.4. Freundlich Adsorption Isotherm for nanokaolin

The adsorption isotherm was applied for adsorption of different dyes on nanokaolin by drawing the relation between $\ln C_e$ and $\ln q_e$ Fig. (12) The slope of the resulting straight line is equals to $1/n$, while the intercept equals to $\ln K_F$. The data obtained for Freundlich isotherm model for DGB and MO37 are collected in Table 7 and 8. The calculated Freundlich isotherm constants and the corresponding coefficient of correlation values are shown in Table 10. The coefficient of correlation was high (R^2 values are 0.955 and 0.931) indicating a good linearity. The results show that the values of n are greater than unity (n) indicating that antibiotic is favorably adsorbed on MO37 and DGB. of Freundlich constants indicate easy uptake of dye from aqueous solution.

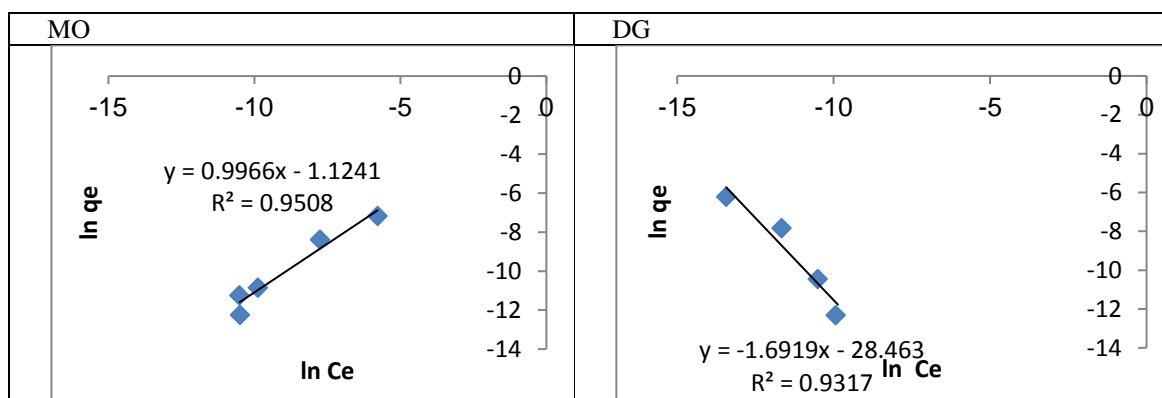


Fig (12): Freundlich isotherm DGB and MO37 on nanokaolin

Table 10: Freundlich equation parameters for nanokaolin

Azo-Dye	Slope	Intercept	K_F	n	R^2
MO37	0.996586	-1.12405	0.32496	-0.00042	0.950
DGB	-1.69193	-28.4629	4.352E-13	-2.4E-07	0.931

5. Kinetic Studies

The pseudo-first order equation is generally expressed as follows [35]:

$$\log(q_e - q_t) = \log q_e - \left(\frac{k_1}{2.303}\right)t$$

where q_e and q_t are the sorption capacities at equilibrium and at time t , respectively (mg g⁻¹) and k_1 (min⁻¹) is the rate constant. The equation applicable to experimental results generally differs from a true first order equation in two ways: (i) the parameter $\log(q_e - q_t)$ does not represent the number of available sites and (ii) the parameter $\log(q_e)$ is an adjustable parameter and often

it is found not equal to the intercept of a plot of $\log(q_e - q_t)$ against t , whereas in a true first order $\log(q_e)$ should be equal to the intercept of a plot of $\log(q_e - q_t)$ against t . In order to fit the pseudo-first order equation to experimental data, the equilibrium capacity, q_e must be known.

On the other hand, if the rate of degradation is a second-order mechanism, the pseudo-second order kinetic rate equation is expressed as:

$$\frac{t}{q_t} = \frac{1}{k_2 q_e^2} + \frac{1}{q_e} t$$

where q_e and q_t are the sorption capacities at equilibrium and at time t , respectively (mg g⁻¹) and k is the

rate constant of pseudo-second order reaction ($g\ mg^{-1}\ min^{-1}$).

If pseudo-second-order kinetics are applicable, the plot of t/q_t against t should give a linear relationship, from

which q_e and k_2 can be determined from the slope and intercept of the plot.

Table 11: Photodegradation parameters of dyes on nanokaolin

Dyes	Log($q_e - q_t$)	t(min)
DGB	-2	15
	-2.3	30
	-2.3	45
	-2.6	60
MO37	-2.10	15
	-2.30	30
	-2.60	45
	-3	60

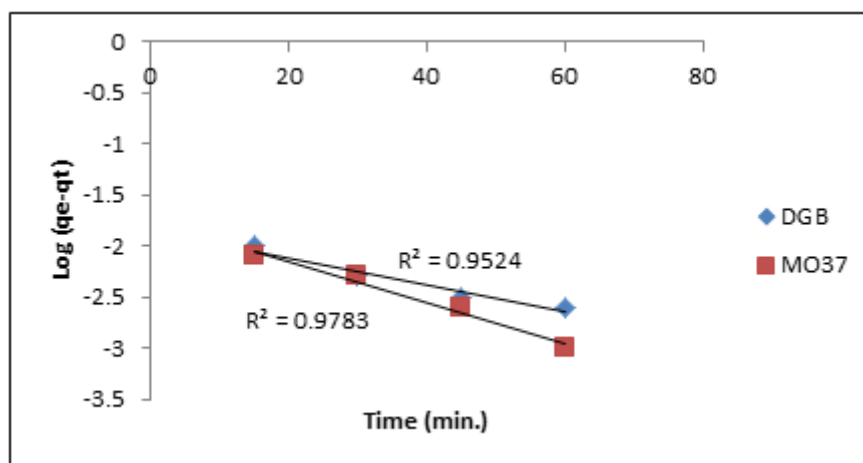


Fig. (13): The pseudo-first order for DGB and MO37 on nanokaolin

6. Conclusions

Heterogeneous photocatalysis using kaolin nanoparticles as photocatalyst was proven to be an effective method for the degradation of DGB and MO37 in its aqueous solution. The experimental results demonstrated that increasing the substrate concentration, light exposure period, and kaolin dosage in an appropriate range contributed to the photocatalytic degradation of DGB and MO37. The removal of the dyes by adsorption on kaolin nanoparticles was found to follow Freundlich isotherm model. The rate of photodegradation follows first order

with a rate constant 0.0101 and 0.073 min^{-1} for DGB and MO37 respectively.

7. Recommendations

- The presence of azo-dyes compounds is a real challenge that has to be faced, it is recommended to eliminate those compounds using nanokaolin in wastewater treatment plants especially that are receiving industrial wastewater.
- Further studies can be done in the field of nano-size particles that can be used for elimination of similar industrial wastes.

References

- 1- R. sanghi , B. bhattacharya ,adsorption-coagulation for the decolorisation of textile dye solutions, water quality research journal. canada, volume 38, no. 3, Pages 553–562, 2003.
- 2-B.K. Nandi, A. Goswami, M.K Purkait ,Removal of cationic dyes from aqueous solutions by kaolin: Kinetic and equilibrium studies, Applied Clay Science, Volume 42, Issues 3–4, Pages 583–590, 2009.
- 3- Jm. Chern , S. huang, study of nonlinear wave propagation theory1. Dye adsorption by activated

- carbon. industrial engineering chemistry research, 37 Pages 253–257, 2005.
- 4- Ho. ys , G. mckay , two stage batch sorption optimized design for dye removal to minimize contact time. *Process safety environmental protection*, 76(4), Pages 313–318, 1998.
 - 5- A. reife , HS. Freeman, environmental chemistry of dyes and pigments. John wiley and sons, n.y. Pages 3–31,1996.
 - 6- R. Sachin ,A. Shirsath, p. Anup , A.Patila, R. Patild , B. J.Naikd, R.Parag , H. GogateShirish and B. Sonawane, Removal of Brilliant Green from wastewater using conventional and ultrasonically prepared poly(acrylic acid) hydrogel loaded with kaolin clay: A comparative study,*Ultrasonics Sonochemistry*, Volume 20, Issue 3, Pages 914–92, 2013.
 - 7- W.chu , dye removal from textile dye wastewater using recycled alum sludge. *water research*, 35(13) Pages 3147–3152, 2001 .
 - 8- G.Crini, Non-conventional low-cost adsorbents for dye removal, *Bioresource Technology*, Volume 97, Issue 9, Pages 1061–1085, June 2006.
 - 9- J.Shore. Dyeing with reactive dyes. In: *Cellulosics Dyeing*. Oxford, Manchester, UK: The Alden Press, 1995.
 - 10- PC. Vandevivere, R. Bianchi, W.Verstraete. Treatment and reuse of wastewater from the textile wet-processing industry: Review of emerging technologies. *Journal of Chemical Technology and Biotechnology*, 72, Pages 289–302, 1998.
 - 11- R. Shertate and P.Thorat, Biotransformation of a Textile Azo Dye Mordant Orange 1 by *Halobacillus Trueperi* Mo-22 in Marine Condition, *International Journal of Pharmaceutical and Phytopharmacology Research*, 3 (4):Pages 268-276,2014.
 - 12- CM. Carliell, SJ.Barclay et al ,Microbial decolorisation of a reactive azo dye under anaerobic conditions, *Water SA*, 21(1) Pages 61–9,1995.
 - 13- J. Easton, “The dye maker’s view. In: Cooper P, editor *Colour in dye house effluent*” Bradford, UK: Society of Dyers and Colourists, Pages11, 1995.
 - 14- RJ. Maguire , Occurrence and persistence of dyes in a Canadian river ,*Water Science Technology*, 25 Pages 265–70, 1992.
 - 15- A. Tripathi, SK.Shrivastava, Ecofriendly treatment of azo dyes – Biodecolorization using bacterial strains, *International Journal of Bioscience, Biochemistry and Bioinformatics*, Vol.1, no.1: pages. 37 – 40, 2011.
 - 16- I. Ayadi, Y. Souissi, I. Jlassi, F. Peixoto, W. Mnif , Chemical Synonyms, Molecular Structure and Toxicological Risk Assessment of Synthetic Textile Dyes: A Critical Review. *Journal of Developed Drugs*, 5 Pages 151, 2016.
 - 17- T.Mustafa ,Yagub,T. Sen, S. Afroze , H.M. Ang, Dye and its removal from aqueous solution by adsorption: A review,*Advances in Colloid and Interface Science*, Volume 209, Pages 172–184, July 2014.
 - 18- DT. Sponza, M. Isik , Toxicity and intermediates of C.I. Direct Red 28 dye through sequential anaerobic/aerobic treatment. *Process Biochemistry*, 40: Pages 2735-2744, 2005.
 - 19- K.Lu, XL. Zhang, YL. Zhao, Wu. ZL , Removal of color from textile dyeing wastewater by foam separation. *Journal of Hazardous Material*, 182, Pages 928-932, 2010.
 - 20- ME.Nagel-Hassemer ,CRS. Carvalho-Pinto, WG.Matias ,FR. Lapolli , Removal of coloured compounds from textile industry effluents by UV/H₂O₂ advanced oxidation and toxicity evaluation. *Environmental Technology*, 32, Pages 1867-1874, 2011.
 - 21- A.Usmani, M. Khan, H.Imran; A. Bhat, , S. Pillai,K. Renjith;M.Ahmad, M. Mohamad Haafiz, Oves, Mohammad,Current Trend in the Application of Nanoparticles for Waste Water Treatment and Purification: Current Organic Synthesis, Volume 14, Number 2,(21) pages 206-226, 2017.
 - 22- W.Xu. G. Zhang, G. Zou, S. Li, X. Liu, Determination of selected antibiotics in the Victoria Harbour and the PearlRiver, South China using high-performance liquid chromatography–electrospray ionization tandem mass spectrometry. *Environmental Pollution*, 145 , Pages 672–679, 2007.
 - 23- D.W. Kolpin, E.T. Furlong, M.T. Meyer, Pharmaceuticals, hormones, and other organic wastewater contaminants in US streams, a national reconnaissance. *Environmental Science and Technology*, 36 Pages 1202–1211, 2000.
 - 24- S.C. Kim, K.Carlson, Temporal and spatial trends in the occurrence of human and veterinary antibiotics in aqueous and river sediment matrices. *Environmental Science and Technology*, 41 Pages 50–57,2007.
 - 25- K. Kummerer, Significance of antibiotics in the environment. *Journal of Antimicrobial Chemotherapy*, 52, Pages 5–7, 2003.
 - 26-S.B. Levy, D.J. Chadwick, F. Eds Goode.; Antibiotic resistance: an ecological imbalance. In *Antibiotic Resistance:Origins, Evolution, Selection and Spread*; Wiley: Chichester. Pages 1–14.1997.
 - 27- F. Baquero, M.C.Negri, M.I. Morosini, J. Blazquez, The antibiotic selective process: concentration-specific amplification of low level resistant populations. In *Antibiotic Resistance: Origins, Evolution, Selection and Spread*, Wiley: Chichester. Pages 93–105.1997.
 - 28- M. Loke, J. Tjornelund, B. Halling-Sorensen, Determination of the distribution coefficient (log K_d) of oxytetracycline, tylosin a, olaquinox, and metronidazole in manure. *Chemosphere*, 48, Pages 351–361, 2002.
 - 29-K. Kumar, S.C. Gupta, Y. Chander, A.K. Singh, Antibiotic use in agriculture and its impact on the terrestrial. *Advances in Agronomy*, 87, Pages 1–54, 2005.
 - 30- Y. Chander, K. Kumar, S.M. Goyal, S.C. Gupta, Antibacterial activity of soil- bound antibiotics.

journal environmental quality, 34, Pages 1952–1957, 2005.

- 31- I. Chopra, M. Roberts, Tetracycline antibiotics: mode of action, applications, molecular biology, and epidemiology of bacterial resistance. *Molecular and Biochemical Parasitology Journal*, 65, Pages 232–260, 2001.
- 32- T. Berger, M. Sterrer, O. Diwald, E. Kno1zinger, D. Panayotov, T.L. Thompson, J.T. Yates Jr, Light-induced charge separation in anatase TiO₂ particles, *Journal Physical Chemistry*, 109 Pages 6061–6068, 2005.
- 33- F.B. Li, X.Z. Li, M.F. Hou, K.W. Cheah, W.C.H. Choy, Enhanced photocatalytic activity of Ce³⁺–TiO₂ for 2-mercaptobenzothiazole degradation in aqueous sus-pension for odour control, *Applied Catalysis*, 285 Pages 181–189, 2005.
- 34- M.S. Norhasri, M.S. Hamidah, A.G. Abd Halim and A. M. Fad Zil, Sol Gel Characterization of Nano Kaoline, *Advanced Materials Research*, 856 Pages 285-289, 2014.
- 35- J. M. Chern, C. Y. Wu, Desorption of dye from activated carbon beds: effects of temperature, pH and alcohol, *Water Research*, 35 Pages 4159–4165, 2001.